# Long-distance entanglement and quantum teleportation in coupled cavity arrays

Salvatore M. Giampaolo[1,2] and Fabrizio Illuminati[1,2,3,4]
[1]Dipartimento di Matematica e Informatica, Università degli Studi di Salerno, Via Ponte don Melillo, I-84084 Fisciano (SA), Italy
[2]CNR-INFM Coherentia, and INFN Sezione di Napoli, Gruppo collegato di Salerno, I-84084 Fisciano (SA), Italy
[3]ISI Foundation for Scientific Interchange, Viale Settimio Severo 65, 00173 Torino, Italy
[4]Corresponding author. Electronic address: illuminati@sa.infn.it
(Dated: October 21, 2009)

We introduce quantum spin models whose ground states allow for sizeable entanglement between distant spins. We discuss how spin models with global end-to-end entanglement realize quantum teleportation channels with optimal compromise between scalability and resilience to thermal decoherence, and can be implemented straightforwardly in suitably engineered arrays of coupled optical cavities.

PACS numbers: 03.65.Ca, 03.67.Mn, 73.43.Nq, 75.10.Jm



Experimental realizations of quantum communication [1] and information [2] protocols fall roughly in two classes. The first one includes all-optical implementations, either with single photons [3, 4, 5], or with continuous variables [6]. In the optical setting, quantum communication is to a great extent decoherence-free and can be easily carried out over long distances. However, the scalability of all-optical devices is fundamentally limited, as the engineering of strong interactions between photons poses formidable challenges. The second class includes matter-based devices such as systems of trapped ions [7, 8], superconducting quantum dots [9], and NMR-based devices [10, 11]. Matter-based implementations, that in principle are easily scalable, suffer from hardly avoidable strong incoherent interactions with the environment. Moreover, typical schemes of quantum communication rely on properly engineered direct interactions between microscopic constituents. This requirement is due to the fact that in many-body systems and spin chains, entanglement between individual constituents decays very rapidly with the distance.

Crucial theoretical progress has been obtained with the recent discovery that the ground state of particular classes of quantum spin models with a finite correlation length can sustain "long-distance entanglement" (LDE), i.e. finite and large values of the entanglement between distant spins even in the thermodynamic limit [12, 13]. The LDE property, being a global, non perturbative, ground-state feature is generated physically over extremely short time scales (instantaneous, to all practical purposes). Moreover, in a particular class of models that will be introduced and discussed in the present work, LDE is enormously stable against thermal fluctuations and decoherence. As we will show, global LDE in these models is achieved by a minimal set of local actions on the end-bond and near-end-bond couplings. Therefore, these models can be realized in physical systems that allow a sufficient degree of control, flexibility, and single-site addressing. Quite recently, hybrid atom-optical systems of coupled cavity arrays (CCAs) have been intensively studied in relation to their ability to realize/simulate collective phenomena typical of strongly correlated systems [14, 15, 16, 17, 18]. In fact, the extremely high controllability, the straightforward addressability of single constituents, and the great degree of flexibility in their geometric design [19], make CCAs strong candidates for the realization of extended communication networks and scalable computational devices.

In this work we investigate quantum spin systems and schemes for the realization of long-distance quantum teleportation based on the phenomenon of LDE, and we illustrate their experimental feasibility in suitably engineered CCAs. We first introduce a class of spin models with open ends and suitably defined end-bond and near-end-bond interactions, and we discuss how the ground-state structure of these models sustains global LDE and allows for long-distance and high-fidelity end-to-end teleportation, even at moderately high temperatures. We then show how these quantum spin channels, that conjugate scalability and resilience to decoherence, can be implemented by open-end, one-dimensional CCAs with properly engineered local couplings at each end. Finally, by exploiting the high degree of control and flexibility of CCAs, we introduce quasi-deterministic schemes of teleportation with high success rates without direct projection on Bell states and Bell measurements, thus overcoming one of the major difficulties that typically beset matter-based devices.

Let us first consider quantum spin models defined on a one-dimensional lattice of length $N$, with open ends, and general site-dependent nearest-neighbor interactions of the $XX$ type:

$$H_s = -\sum_{k=1}^{N-1} J_k (S_k^x S_{k+1}^x + S_k^y S_{k+1}^y) \, , \qquad (1)$$

where $J_k$ is the set of the $N-1$ nearest-neighbor couplings and $S_k^\alpha$ denotes the Spin-1/2 operators at site $k$ ($\alpha = x, y$). The pure $XX$ limit is recovered when $J_k = J, \forall k$. The model is exactly solvable by Jordan-Wigner diagonalization, both for chains of finite size and in the thermodynamic limit [20]. For arbitrary site-dependent couplings, the associated models are still exactly solvable by a straightforward extension of the techniques developed in Ref. [20], albeit, in general, only numerically [13, 21, 22]. For these models, the phenomenon of perfect ground-state LDE (maximal end-to-end concurrence independent of the size of the chain) sets on when the Hamil-

tonian $H_s$ is dimerized, with perfectly alternated weak and strong couplings: $J_k \equiv J_{odd}$ ($k = 1, 3, ..., N-1$), $J_k \equiv J_{even}$ ($k = 2, 4, ..., N-2$), and $J_{odd} \ll J_{even}$ [13]. Normalizing all couplings by $J_{even}$, and renaming the rescaled odd coupling: $J_{odd}/J_{even} \equiv \lambda$, the condition for perfect LDE reads $\lambda \ll 1$ [13]. Ground-state quasi-perfect LDE (maximal end-to-end concurrence slowly decaying with the size of the chain) is realized by models with uniform bulk (b) interactions and weak end bonds (eb): $J_2 = J_3 = ... = J_{N-2} \equiv J_b$, $J_1 = J_{N-1} \equiv J_{eb}$. Rescaling all couplings by $J_b$ (with $J_{eb}/J_b \equiv \lambda$), the condition for quasi-perfect LDE reads $\lambda \ll 1$ [13]. In the first instance (*dimerized $XX$ model*) the energy gap closes exponentially with the size of the system, making this system useless for realistic applications at finite temperature. In the second instance (the $\lambda$ *model*) the gap closes with an algebraic power law, but useful amounts of LDE can survive only at extremely low temperatures, unreachable at present and in the immediately foreseeable future [13]. Here we introduce a $\lambda$-$\mu$ *model* that realizes an optimal compromise between the requirements of strong LDE in a system of large size, robustness of LDE at moderately high temperatures, and ease of realistic implementations. The $\lambda$-$\mu$ model is defined by Hamiltonian (1) with uniform bulk interactions and alternating weak end bonds (eb) and strong near-end bond (neb) interactions: $J_3 = J_4 = ... = J_{N-3} \equiv J_b$, $J_2 = J_{N-2} \equiv J_{neb}$, and $J_1 = J_{N-1} \equiv J_{eb}$. Normalizing all interactions by $J_b$, and redefining the scaled couplings $J_{eb}/J_b \equiv \lambda$ and $J_{neb}/J_b \equiv \mu$, the condition for an optimized end-to-end LDE is $\lambda \ll 1 \ll \mu$.

The LDE properties of the $\lambda$-$\mu$ chain, at zero and finite temperature, are reported in the upper panel of Fig. 1, where the end-to-end concurrence is plotted as a function of the size of the chain. In the lower panel of Fig. 1 we report the behavior of the corresponding maximal fidelity of teleportation $\mathcal{F}_{max}$, which, in the case of nonvanishing spin-spin concurrence, is a monotonic function of the pairwise end-to-end entanglement [13, 23]. Fig. 1 shows that interacting spin systems of the $\lambda$-$\mu$ type conjugate efficiently resilience to decoherence and scalability, as further confirmed by comparing with the performance of systems of the $\lambda$ type.

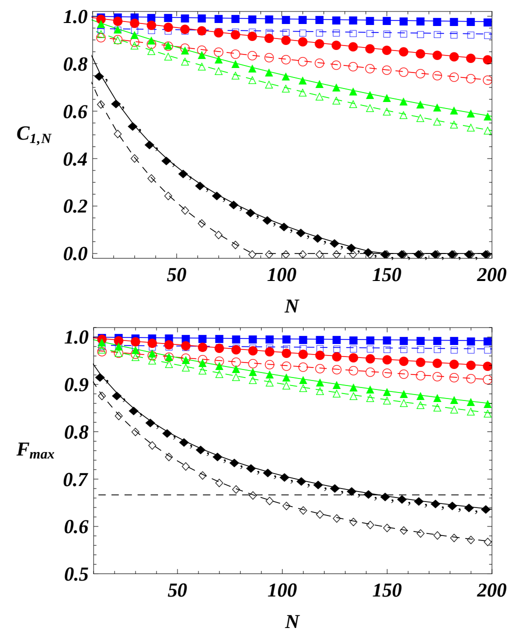


FIG. 1: (Color online) Upper panel, lines with full symbols: Concurrence $\mathcal{C}_{1N}$ between the end points of a $\lambda$-$\mu$ chain as a function of the length $N$, for different values of $\lambda$ and $\mu$, at zero temperature. From top to bottom: Line with full boxes: $\lambda = 0.15$, $\mu = 7.0$. Full circles: $\lambda = 0.2$, $\mu = 5.0$. Full triangles: $\lambda = 0.4$, $\mu = 3.0$. Full diamonds: $\mathcal{C}_{1N}$ of a $\lambda$ spin chain (i.e. with $\mu = 1$) for $\lambda = 0.2$. Upper panel, lines with empty symbols: $\mathcal{C}_{1N}$ as a function of $N$ at different reduced temperatures $T/J_b$ for the same sets of values of $\lambda$ and $\mu$ as for the corresponding lines with full symbols. From top to bottom: Line with empty boxes: $T/J_b = 0.0005$. Empty circles: $T/J_b = 0.0001$. Empty triangles: $T/J_b = 0.001$. Empty diamonds: $\mathcal{C}_{1N}$ of the corresponding $\lambda$ spin chain at $T/J_b = 0.0006$. Lower Panel: The maximal fidelity of teleportation $\mathcal{F}_{max}$ [23] between the end points of the $\lambda$-$\mu$ chain as a function of $N$, at zero and finite temperature, for the same set of values reported in the upper panel. In the case of the $\lambda$ model (lines with diamonds), $\mathcal{F}_{max}$ sinks below the classical threshold $2/3$ (horizontal dashed line), for the corresponding vanishing values of the end-to-end concurrence (See upper panel). All quantities being plotted are dimensionless.

Let us now consider a linear CCA with open ends, consisting of $N$ cavities. The dynamics of a single constituent of the array doped with a single two-level atom is well described by the Jaynes-Cummings Hamiltonian

$$H_k = \omega a_k^\dagger a_k + \omega' |e_k\rangle\langle e_k| + g a_k^\dagger |g_k\rangle\langle e_k| + g|e_k\rangle\langle a_k| a_k \,, \quad (2)$$

where $a_k$ ($a_k^\dagger$) is the annihilation (creation) operator of photons with energy $\omega$ in the $k$-th cavity, $|g_k\rangle$ and $|e_k\rangle$ are respectively the ground and excited atomic states, separated by the gap $\omega'$, and $g$ is the photon-atom coupling strength. The local Hamiltonian Eq. (2) is immediately diagonalized in the basis of dressed photonic and atomic excitations (polaritons):

$$\begin{aligned} |\emptyset_k\rangle &= |g_k\rangle|0_k\rangle \,; & (3)\\ |n+_k\rangle &= \cos\theta_n |g_k\rangle|n_k\rangle + \sin\theta_n |e_k\rangle|(n-1)_k\rangle \quad n \geq 1 \,; \\ |n-_k\rangle &= \sin\theta_n |g_k\rangle|n_k\rangle - \cos\theta_n |e_k\rangle|(n-1)_k\rangle \quad n \geq 1 \,, \end{aligned}$$

where $\theta_n$ is given by $\tan 2\theta_n = -g\sqrt{n}/\Delta$ and $\Delta = \omega' - \omega$ is the atom-light detuning. Each polariton is characterized by an energy equal to

$$\varepsilon_0 = 0; \qquad \varepsilon_{n\pm} = n\omega \pm \sqrt{ng^2 + \Delta^2} \,. \quad (4)$$

When $\omega = \sqrt{g^2 + \Delta^2}$ the ground state of Eq. (2) becomes two-fold degenerate, resulting in a superposition of $|\emptyset_k\rangle$ and $|1-_k\rangle$, see Fig. 2. If both the atom-cavity interaction energy and the working temperature are small compared to $\varepsilon_{2-} = 2\sqrt{g^2 + \Delta^2} - \sqrt{2g^2 + \Delta^2}$, one may neglect all the local polaritonic states but $|\emptyset_k\rangle$ and $|1-_k\rangle$. This situation defines a local two-level system. Adjacent cavities can be easily coupled either by photon hopping or via wave guides of different dielectric and conducting properties. The wave function overlap between adjacent cavities introduces the associated tunneling

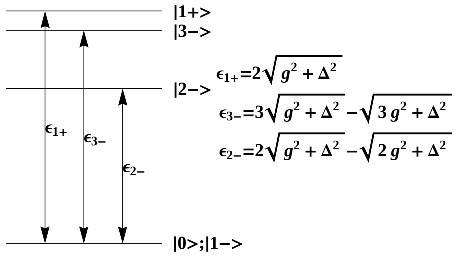


FIG. 2: Representation of the energy levels for a cavity with $\omega = \sqrt{g^2+\Delta^2}$. The ground state is two-fold degenerate, and the energy gap $\varepsilon_{2-}$ prevents the occupancy of the higher energy levels, thus realizing an effective two-level system.

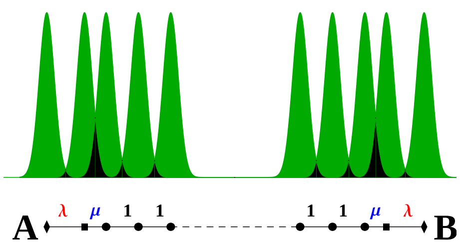


FIG. 3: (Color online) Scheme of a CCA realizing the $\lambda$-$\mu$ $XX$ model. Dark green (grey in black and white print): Overlap of the wave functions associated to each site of the array. The two next-to-end sites (boxes) are symmetrically displaced towards their neighbors in the bulk (circles). The overlap (black area) between the wave functions of these two cavities and their neighbors in the bulk is thus larger than the would-be reference (unit) one in an equispaced CCA. Viceversa, the overlap between the end sites of the array (diamonds) and the next-to-end sites is reduced proportionally compared to an equispaced array.

elements, so that the total Hamiltonian of the CCA is

$$H_{cca} = \sum_k^N H_k - \sum_k^{N-1} J_k (a_k^\dagger a_{k+1} + a_{k+1}^\dagger a_k) \; . \qquad (5)$$

Each hopping amplitude $J_k$ depends strongly on both the geometry of the cavities and the actual overlap between adjacent cavities. If the maximum value among all the couplings $\{J_k\}$ is much below the energy of the first excited state: $\max\{J_k\} \ll \varepsilon_{2-}$, then the total Hamiltonian Eq. (5) can be mapped in a spin-1/2 model of the $XX$ type with site-dependent couplings of the form Eq. (1), where the state $|\emptyset_k\rangle$ ($|1-_k\rangle$) plays the role of $|\downarrow_k\rangle$ ($|\uparrow_k\rangle$). The mapping to an open-end $\lambda$-$\mu$ linear spin chain is then realized, e.g., by simply tuning the distance between the end- and next-to-end sites of the CCA, as showed in Fig. 3. The $\lambda$-$\mu$ chain is thus realized by placing the second and the $(N-1)-th$ cavities slightly off their would-be positions in an equispaced CCA. This shift lowers the coupling between the two cavities and those at the end-points of the chain: $J_1/J_b = J_{N-1}/J_b = \lambda < 1$, where $J_b$ is the uniform nearest-neighbor coupling in the bulk. Viceversa, it increases the coupling between the two next-to-end sites and their nearest neighbors in the bulk: $J_2/J_b = J_{N-2}/J_b = \mu > 1$.

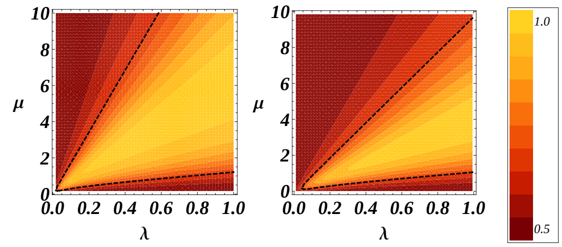


FIG. 4: (Color online) Fidelity of teleportation $F_{max}$ in a $\lambda$-$\mu$ configuration, by exact numerical diagonalization, for a CCA of $N = 12$ cavities, as a function of the couplings $\lambda = J_1/J_b$ and $\mu = J_2/J_b$ and at different temperatures $T/J_b$. Left panel: $T/J_b = 0.005$. Right panel: $T/J_b = 0.01$. $F_{max}$ varies between 0.5 (dark red in color, dark grey in black and white print) and 1.0 (light orange in color, light grey in black and white print). Dashed lines: Classical threshold $F_{max}^c = 2/3$. All quantities being plotted are dimensionless.

We now proceed to illustrate that CCAs in the $\lambda$-$\mu$ configuration allow for long-distance and high-fidelity quantum communication in fully realistic conditions at moderately high temperatures. In Fig. 4 we report the fidelity of teleportation $F_{max}$ as a function of the reduced couplings $\lambda$ and $\mu$ for different temperatures. Remarkably, Fig. 4 shows the existence of a rather high *critical* temperature of teleportation for CCAs in the $\lambda$-$\mu$ configuration. The region of the physical parameters compatible with a nonclassical fidelity $F_{max} > 2/3$ is progressively reduced with increasing temperature, until it disappears at $T_c \approx 0.13J_b$. Similar behaviors are observed for longer CCAs, with $T_c$ slowly decreasing with the length of the array. For instance, for an array of $N = 36$ cavities in the $\lambda$-$\mu$ configuration, the critical temperature of transition to *bona fide* quantum teleportation is $T_c \approx 0.11J_b$.

A formidable obstacle to the concrete realization of working quantum teleportation devices is performing the projection over a Bell state, in order for the sender to teleport a quantum state faithfully to the receiver. In fact, in the framework of condensed matter there hardly exist quantities, easily available in current and foreseeable experiments, that admit as eigenstates any two-qubit Bell states. In the following, we will illustrate a simple and concrete scheme for long-distance, high-fidelity quantum teleportation in $\lambda$-$\mu$ CCAs that realizes Bell-state projections indirectly, by matching together free evolutions and local measurements of easily controllable experimental quantities [24, 25, 26]. We first illustrate it in the simplest case of two cavities at zero temperature, with the first cavity accessible by the sender and the second one by the receiver. The sender has access also to a third cavity, the "0" cavity, that is decoupled from the rest of the chain and stores the state to be teleported $|\varphi\rangle = \alpha|\uparrow_0\rangle + \beta|\downarrow_0\rangle$. The decoupling of the 0-th cavity is achieved, e. g., by removing the degeneracy among $|0\rangle_0$ and $|1-\rangle_0$ and taking $|\varepsilon_0 - \varepsilon_{1-}| \gg J_0$.

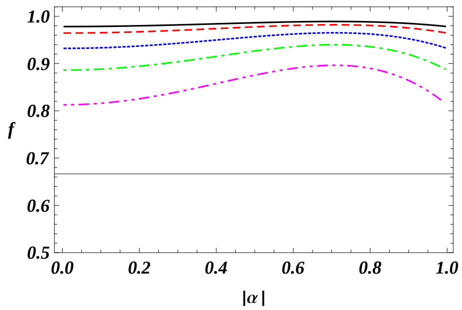


FIG. 5: (Color online) Fidelity of teleportation $f$ in a $\lambda$-$\mu$ CCA channel of $N = 12$ cavities, for a generic input $|\varphi\rangle = \alpha|\uparrow_0\rangle + \beta|\downarrow_0\rangle$, as a function of $|\alpha|$ at different temperatures. From top to bottom: Solid line: $T = 0.001 J_b$. Dashed line: $T = 0.003 J_b$. Dotted line: $T = 0.004 J_b$. Dot-dashed line: $T = 0.005 J_b$. Double-dot-dashed line: $T = 0.007 J_b$. Here $\lambda = 0.5$, $\mu = 4.0$, and $\nu = 50$. Horizontal solid line: Classical threshold $f_c = 2/3$. All quantities being plotted are dimensionless.

The total system is initially in the state

$$|\Psi(0)\rangle = \frac{1}{\sqrt{2}}(\alpha|\uparrow_0\rangle + \beta|\downarrow_0\rangle)(|\uparrow_1\rangle|\downarrow_2\rangle + |\downarrow_1\rangle|\uparrow_2\rangle). \quad (6)$$

At $t = 0$ the state begins to evolve and, if $J_0 \gg J_1$, one has:

$$\begin{aligned} |\Psi(t)\rangle \;=\; & \frac{1}{\sqrt{2}}\left[\alpha|\uparrow_0\rangle|\uparrow_1\rangle|\downarrow_2\rangle + \beta|\downarrow_0\rangle|\downarrow_1\rangle|\uparrow_2\rangle\right. \quad (7) \\ & |\uparrow_0\rangle|\downarrow_1\rangle(\alpha\cos(J_0 t)|\uparrow_2\rangle - i\beta\sin(J_0 t)|\downarrow_2\rangle) \\ & \left.|\downarrow_0\rangle|\uparrow_1\rangle(-i\alpha\sin(J_0 t)|\uparrow_2\rangle + \beta\cos(J_0 t)|\downarrow_2\rangle)\right]. \end{aligned}$$

If at time $t = \pi/(4J_0)$ Alice measures the local magnetizations ($S_0^z$, $S_1^z$) in the first two cavities, she will find with probability $1/2$ that the teleported state is the image of $|\varphi\rangle$ under a local rotation. The value $1/2$ for the probability stems from the fact that any simultaneous eigenstate of $S_0^z$ and $S_1^z$ can be obtained with equal probability but one may discard the case in which the total magnetization is equal to $\pm 1$. Realizing a local rotation of $\pm\pi/2$ around $S_2^z$, with the sign depending on the result of the measurement that the sender communicates classically to the receiver, the latter recovers the original state $|\varphi\rangle$ with unit fidelity.

The simple protocol described above can be immediately extended to $\lambda$-$\mu$ CCAs of any size, at finite temperature, and removing the constraint $J_1 \ll J_0$. By resorting again to exact diagonalization, in Fig. 5 we report the behavior of the fidelity of teleportation $f$, as a function of $|\alpha|$ of the state $|\varphi\rangle$, in the case of an array of $N = 12$ cavities, with $\nu \equiv J_0/J_b = 50$ and for different temperatures. Also in the non-ideal case the teleportation protocol has probability 1/2 of success. The fidelity depends on the input state, with a maximum for inputs with $|\alpha| = |\beta| = 1/\sqrt{2}$ and a minimum for inputs with $|\alpha| = 0.1$. The fidelity remains above 0.95 for all values of $|\alpha|$ at moderately low temperatures ($T \simeq 10^{-3} J_b$).

In conclusion, we have introduced a class of quantum spin models characterized by a non-perturbative, ground-state (quasi) long-distance entanglement strongly resilient to thermal decoherence, that can be efficiently realized with a minimal set of local actions on the end sites of open CCAs. We have showed that these systems allow for a simple probabilistic protocol of long-distance, high-fidelity quantum teleportation that yields a high rate of success without direct Bell measurements and projections over Bell states. We acknowledge financial support from the EC under the FP7 STREP Project HIP, Grant Agreement n. 221889, from MIUR under the FARB fund, and from INFN under Iniziativa Specifica PG 62. F. I. acknowledges support from the ISI Foundation for Scientific Interchange.


[1] C. H. Bennett, G. Brassard, C. Crépeau, R. Jozsa, A. Peres, and W. K. Wootters, Phys. Rev. Lett. **70**, 1895 (1993).
[2] M. A. Nielsen and I. L. Chuang, *Quantum Computation and Quantum Information* (Cambridge University Press, Cambridge, 2000).
[3] D. Bouwmeester, J.-W. Pan, K. Mattle, M. Eibl, H. Weinfurter, and A. Zeilinger, Nature **390**, 575 (1997).
[4] D. Boschi, S. Branca, F. De Martini, L. Hardy, and S. Popescu, Phys. Rev. Lett. **80**, 1121 (1998);
[5] R. Ursin *et al.*, Nature **430**, 849 (2004).
[6] H. Yonezawa, T. Aoki, and A. Furusawa, Nature **431**, 430 (2004).
[7] M. Riebe *et al.*, Nature **429**, 734 (2004).
[8] M. D. Barrett *et al.*, Nature **429**, 737 (2004).
[9] D. Fattal, E. Diamanti, K. Inoue, and Y. Yamamoto, Phys. Rev. Lett. **92**, 037904 (2004).
[10] M. A. Nielsen, E. Knill, and R. Laflamme, Nature **395**, (1998).
[11] G. Brassard, S. L. Braunstein, and R. Cleve, Physica D **120**, 43 (1998).
[12] L. Campos Venuti, C. Degli Esposti Boschi, and M. Roncaglia, Phys. Rev. Lett. **96**, 247206 (2006); Phys. Rev. Lett. **99**, 060401 (2007).
[13] L. Campos Venuti, S. M. Giampaolo, F. Illuminati, and P. Zanardi, Phys. Rev. A **76**, 052328 (2007).
[14] M. J. Hartmann, F. G. S. L. Brandão, and M. B. Plenio, Nature Phys. **2**, 849 (2006).
[15] A. D. Greentree, C. Tahan, J. H. Cole, and L. C. L. Hollenberg, Nature Phys. **2**, 856 (2006).
[16] D. G. Angelakis, M. F. Santos, and S. Bose, Phys. Rev. A **76**, 031805(R) (2007).
[17] D. Rossini and R. Fazio, Phys. Rev. Lett. **99**, 186401 (2007).
[18] M. J. Hartmann, F. G. S. L. Brandão, and M. B. Plenio, Phys. Rev. Lett. **99**, 160501 (2007).
[19] M. J. Hartmann, F. G. S. L. Brandão, and M. B. Plenio, Laser & Photon. Rev. **2**, 527 (2008).
[20] E. Lieb, T. Schultz, and D. Mattis, Ann. Phys. (N.Y.) **16**, 407 (1961).
[21] S. M. Giampaolo and F. Illuminati, unpublished.
[22] A. Wojcik *et al.*, Phys. Rev. A **72**, 034303 (2005).
[23] M. Horodecki, P. Horodecki, and R. Horodecki, Phys. Rev. A. **60**, 1888 (1999); P. Badziag, M. Horodecki, P. Horodecki, and R. Horodecki, Phys. Rev. A **62**, 012311 (2000)
[24] S.-B. Zheng, Phys. Rev. A **69**, 064302 (2004).
[25] L. Ye and G-C. Guo, Phys. Rev. A **70**, 054303 (2004).
[26] W. B. Cardoso, A. T. Avelar, B. Baseia, and N. G. de Almeida, Phys. Rev. A **72**, 045802 (2005).